

Organic electrochemical transistors as novel biosensing platforms to study the electrical response of whole blood and plasma

Original

Organic electrochemical transistors as novel biosensing platforms to study the electrical response of whole blood and plasma / Preziosi, V.; Barra, M.; Tomaiuolo, G.; D'Angelo, P.; Marasso, S. L.; Verna, A.; Cocuzza, M.; Cassinese, A.; Guido, S.. - In: JOURNAL OF MATERIALS CHEMISTRY. B. - ISSN 2050-750X. - ELETTRONICO. - 10:1(2022), pp. 87-95. [10.1039/d1tb01584b]

Availability:

This version is available at: 11583/2958660 since: 2022-03-21T08:02:30Z

Publisher:

Royal Society of Chemistry

Published

DOI:10.1039/d1tb01584b

Terms of use:

This article is made available under terms and conditions as specified in the corresponding bibliographic description in the repository

Publisher copyright

(Article begins on next page)

Journal of Materials Chemistry B

Materials for biology and medicine

Accepted Manuscript

This article can be cited before page numbers have been issued, to do this please use: V. Preziosi, M. Barra, G. Tomaiuolo, P. D'Angelo, S. L. L. Marasso, A. Verna, M. Cocuzza, A. Cassinese and S. Guido, *J. Mater. Chem. B*, 2021, DOI: 10.1039/D1TB01584B.



This is an Accepted Manuscript, which has been through the Royal Society of Chemistry peer review process and has been accepted for publication.

Accepted Manuscripts are published online shortly after acceptance, before technical editing, formatting and proof reading. Using this free service, authors can make their results available to the community, in citable form, before we publish the edited article. We will replace this Accepted Manuscript with the edited and formatted Advance Article as soon as it is available.

You can find more information about Accepted Manuscripts in the [Information for Authors](#).

Please note that technical editing may introduce minor changes to the text and/or graphics, which may alter content. The journal's standard [Terms & Conditions](#) and the [Ethical guidelines](#) still apply. In no event shall the Royal Society of Chemistry be held responsible for any errors or omissions in this Accepted Manuscript or any consequences arising from the use of any information it contains.

ARTICLE

Organic electrochemical transistors as novel biosensing platforms to study the electrical response of whole blood and plasma

Valentina Preziosi,^{a*} Mario Barra,^{b*} Giovanna Tomaiuolo,^a Pasquale D'Angelo,^c Simone Luigi Marasso,^{c,d} Alessio Verna,^d Matteo Cocuzza,^{c,d} Antonio Cassinese^{b,c} and Stefano Guido^{a,f,g}Received 00th January 20xx,
Accepted 00th January 20xx

DOI: 10.1039/x0xx00000x

In this paper, for the first time to our knowledge, organic electrochemical transistors are employed to investigate the electrical response of human blood, plasma and alternative buffer solutions that inhibit red blood cell (RBC) aggregation. Our focus is to select a suitable electrolytic platform and the related operating conditions, where the RBCs effect on the OECT response can be observed separately from the strong ionic environment of plasma in whole blood. The transient response of whole blood to pulse experiments is characterized by two time constants, which can be related to blood viscosity and to the capacitive coupling between the ionic and electronic components of the overall system. The role of capacitive effects, likely due to enhanced double-layer formation by negatively charged RBCs, is also confirmed by the increase of transconductance which was found in RBC suspensions as compared to the suspending buffer. Overall, the complex behavior found in these experiments provides new insights for the development of innovative blood-based sensing devices for biomedical applications.

1. Introduction

Recently, organic thin-film transistors (OTFTs) are attracting increasing attention thanks to their potential as sensors with many advantages, such as real-time analysis, low cost, biocompatibility, flexibility, and ease of integration in lab-on-a-chip devices^{1, 2}. Organic electrochemical transistors (OECTs) - a special class of organic thin-film transistors - are particularly interesting for bioelectronic applications³, being based on the exploitation of conductive polymers as poly(3,4-ethylenedioxythiophene) polystyrene sulfonate (PEDOT:PSS), with mixed ionic-electronic conduction⁴. OECT operation mechanism has been deeply discussed with reference to several kinds of applications⁵⁻⁸. More in general, OECT response with its very high transconductance enables operations at ultra-low voltages in liquids, making them particularly suitable to investigate also cellular systems and living matter⁹. OECTs work as transducers and amplifiers from ionic signals, present in the electrolytic solution, to electronic ones. This feature allows the detection of low concentrations of ionic species, going well

beyond the performances of the currently-available commercial sensors¹⁰⁻¹³.

Such high-sensitive tool and miniaturized devices could be coupled to provide robust platforms representing *in vitro* physio-pathologically relevant microenvironments. These could be able to mimic cell and organ level organizational structures, thanks to their user-defined design, small length scales and optimal control and sensing of mechanical and tissue environment. Taking advantage of microfluidics principles, organ-on-chip devices are integrated platforms consisting of microfluidic channels populated with several cell types to create minimal functional organ units for drug testing and modelling human physiology and disease¹⁴⁻¹⁶. Beyond specific cell lines, blood, i.e. the fluid tissue that delivers oxygen and nutrients to tissues and cells and that is responsible of the immunological response, is the most exploited biological fluid for biomedical applications. Blood is a complex fluid consisting in a suspension of cells, erythrocytes (red blood cells-RBCs), leucocytes (white blood cells-WBCs) and platelets, immersed in a low viscous fluid called plasma¹⁷.

In this scenario, OECTs can be particularly precious, unravelling the issue of blood handling and sensing in integrated microfluidic devices. In particular, RBCs, being the major constituents of blood, are deformable cells that have a great impact on the physiological flow of blood in microvasculature^{18, 19}. Their abnormal shape and concentration, indeed, can lead to organ and tissues disfunction and death²⁰⁻²³. Moreover, plasma, being a water solution of cations like Na⁺, K⁺, Ca²⁺ and Mg²⁺, anions like Cl⁻ and HCO₃⁻, and high molecular weight substances like proteins and lipoproteins, strongly impacts the electrical response of blood^{24, 25}. Since a long time, there has been a lot of interest about the electrical behavior of human blood, in terms,

^aDepartment of Chemical, Materials and Production Engineering - University Federico II – P.le Tecchio 80, I-80125 Naples, Italy

^bCNR-SPIN, c/o Department of Physics "Ettore Pancini", P.le Tecchio, 80, I-80125 Napoli, Italy

^cMEM-CNR, Parco Area delle Scienze 37/A, I-43124 Parma, Italy

^dChi-Lab, Department of Applied Science and Technology, Politecnico di Torino, C.so Duca degli Abruzzi 24, 10129 Torino, Italy

^eDepartment of Physics "Ettore Pancini", University Federico II – P.le Tecchio 80, I-80125 Naples, Italy

^fNational Interuniversity Consortium for Materials Science and Technology (INSTM), 50121 Firenze, Italy

^gCEINGE, Advanced Biotechnologies, 80145 Napoli, Italy

† Footnotes relating to the title and/or authors should appear here.

Electronic Supplementary Information (ESI) available: [details of any supplementary information available should be included here]. See DOI: 10.1039/x0xx00000x

for example, of the conductivity (or its reciprocal, the resistivity), given its strict correlation with blood physiology and the repercussion of blood electrical variations on biomedical devices. In 1873, Maxwell²⁶ published a book containing a theoretical dissertation about the conductivity of a suspension of non-conducting spheres in a conducting medium. Some years later, Hober determined for the first time the different resistivity of blood, at low and high frequencies, due to the presence of a membrane around RBCs.

Later on, Fricke²⁷ first and Velick and Gorin²⁸ then, extended Maxwell's work and applied it to blood, assuming RBCs as non-conducting ellipsoids and plasma as a conductive medium. Other works followed and correlated blood conductivity with the presence of erythrocytes and plasma leading to the conclusion that, even if plasma is a complex fluid full of ionic species, the presence of red cells plays a key role in the electrical response of blood^{29,30}. In particular, some works addressed the change in human blood electrical properties in static conditions due to the haematocrit (*Hct*), i.e. the ratio of volume fraction of the blood cells and the total volume, and to the red blood cell random orientation. Other works instead focused on the effect of RBCs parallel orientation under flow confirming that, even if RBCs display a low conductivity with respect to plasma, their impact cannot be neglected²⁹. Despite all the studies on the electrical properties of human blood, the effect of RBCs in terms of electrical conductivity is still controversial, making the exploitation of blood-based electrical devices still an open issue. In the present work, the problem of the response of OECTs when human blood, plasma and an alternative buffer solution, containing RBCs in suspension are used, is addressed. Building on previous reports by our group on the use of OECTs as sensing devices³¹⁻³⁷ and on the analysis of blood flow in blood-on-chip devices^{38,39}, the main goal of this paper is to exploit OECTs as a reliable platform to distinguish the effect of RBCs from those related to the plasma, which is characterized by a high ionic concentration.

A main challenge associated with running OECTs with blood and RBC suspensions is related to the particulate nature of blood and to the peculiar properties of RBCs, as deformability and cell tendency to aggregate under static or weak flow conditions, as well as to the number of electrolytes present in plasma. Despite the key role that blood could play in integrated devices, no experimental study on the use of OECTs for blood testing has been published so far, to the best of our knowledge. Our approach is based on the exploitation of OECTs with whole blood and RBCs suspensions at different values of hematocrit to separate the effect of RBC and plasma. Different responses have been found in this way.

2. Material and methods

Materials and sample preparation

RBC suspensions. Venous blood samples were withdrawn from healthy volunteers and used within 4 hours of collection. Blood was stored in vials and let it rotate on a blood tube rotator to

avoid cell sedimentation just before the experiment. For whole blood experiments, blood was measured at hematocrit values *Hct* (i.e. RBCs volume fraction) around 40%. In addition to whole blood, suspensions at 25% and 45% of *Hct* have been prepared by diluting RBCs in a 1:100 Anticoagulant Citrate Dextrose (ACD) and Albumin solution. To this end, blood was centrifuged (Hettich Universal 32 R) at 1600 revolutions per minute for 15 min and at 20°C to separate RBCs from other cellular components and plasma. ACD was purchased by Haemonetics (0.6% citric acid, 1.1% anhydrous dextrose, 2.3% sodium citrate, 96% water) and used to avoid clotting. Fetal Bovine Serum (FBS-Albumin) was purchased by Merck and it was dissolved in ACD (4 g in 10 ml ACD) by mixing the solution in a beaker on a magnetic stirrer for about 20 min at room temperature.

Conductance measurements of ACD and ACD plus Albumin solutions, performed by using a conductivity meter (PC 2700, Eutech Instruments), gave values about 14 mS for ACD and 10 mS for ACD plus Albumin. Such values are similar to the typical ones measured for whole blood⁴⁰.

Microscopy imaging

Optical images of whole blood and of RBC suspensions at 25% and 45% were acquired by using an optical inverted microscope (Zeiss Axiovert 100) connected to a videocamera (Phantom 4.3) in bright field using a 40x oil immersion objective (Zeiss).

OECT fabrication

The experimental apparatus used in this work has been described in detail elsewhere^{31,32} and it will be just briefly reviewed here. Device fabrication followed the already reported procedure in^{31,41} (Fig. 1). Electrodes, fabricated by e-beam evaporation (ULVAC EBX-14D), were obtained by depositing Ti/Au film (thickness 10 nm/100 nm) on Si wafer (100) finished with 1 µm of thermal oxide. A 200 nm thick PEDOT:PSS layer (Clevios PH 1000, doped with 5 volume % ethylene glycol, 0.1 volume % dodecyl benzene sulfonic acid, and 1 wt% of GOPS (3-glycidyloxypropyl)trimethoxysilane) was obtained by spin coating on the source and drain electrodes and subsequently patterned via photolithography (Microchemicals AZ9260 resist) and etching with O₂ plasma. A PDMS chamber, with an internal volume of 150 µl, was aligned with the PEDOT:PSS channel and irreversibly bonded on the surface (Fig. 1a). Final device geometry (see Fig. 1b) is characterized by a width to length (W/L) ratio equal to 30 (W = 6 mm, L = 200 µm). In particular, drain and source electrodes are 250 µm in width and 7 mm in length both having a contact pad of 1 mm x 2 mm.

OECT characterization. OECT devices were characterized by using a homemade probe station connected to a two-channels multimeter (Keithley 2612A) and controlled by Labview software. As gate electrode, a gold wire (99.99% Au supplied by Franco Corradi sas) with a diameter of 1 mm was immersed into the electrolyte for the OECT characterization. Hence, in the investigated configuration, the gate electrode was not coplanar with source and drain contacts. Additional measurements were also performed by a platinum wire (99.9% supplied by Franco Corradi sas, with a diameter of 0.6 mm). During the measurements, attention was paid in order to

immerse the same equivalent area (about 8 mm²) for both gold and platinum electrodes.

During the overall time required to complete the OECT measurement protocol (about 30 minutes), we can assume that the RBC were sedimented. However, our experimental findings suggest that the cell sedimentation does not play a significant role on the OECT response, as it will be discussed in the Results section. After each measurement, fresh blood was replaced and all the experiments were carried out at room temperature.

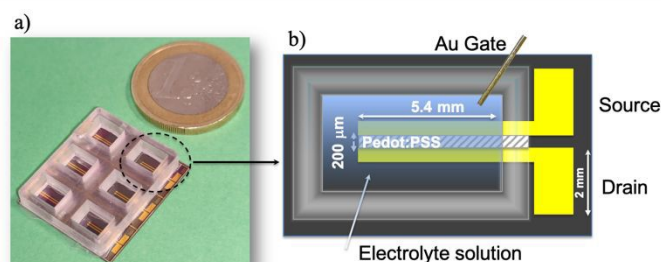


Fig. 1: a) Picture and b) sketch of OECT device.

3. Results and discussion

Microscopy imaging

Fresh venous human blood withdrawn from healthy volunteers has been initially observed at the optical microscope to check its health state. In static conditions, indeed, healthy RBCs assume a biconcave shape with a diameter around 8 μm and, in absence of any anticoagulant, they tend to aggregate and to form microstructures called rouleaux⁴². An optical image of whole blood over time is shown in Fig. 2 where the enhanced presence of rouleaux occurring in the order of seconds from the first acquisition is more and more evident. RBCs have been also observed in ACD plus Albumin solution at two different cell concentrations, 25 and 45%, where cells do not aggregate owing to the presence of the anticoagulant (ACD). Cell viability was also monitored after OECT experiments (about 2 hours after collection) and no cell alteration has been observed (Fig. S1).

OECT response in blood and plasma

In the first part of this work, fresh whole blood and plasma have been analyzed in terms of the related OECT response. Plasma, in particular, was obtained by centrifuging blood from the same donor as described in the Experimental section. The PEDOT:PSS active channel was in contact with about 150 μl of the solution under investigation thanks to a Polydimethylsiloxane (PDMS) well, acting as a fluid reservoir.

Gold gate electrodes were basically considered to study the OECT response. After gate immersion into the reservoir, a positive voltage between gate and source, V_{GS} , was applied in

order to drive the PEDOT:PSS-based OECT operation in the depletion-mode regime¹⁰.

DOI: 10.1039/D1TB01584B

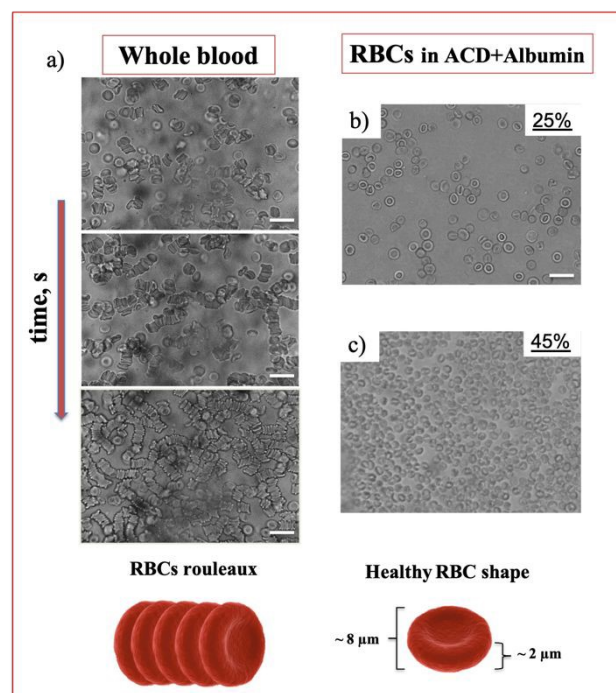


Fig. 2: Optical images of whole blood just after withdrawn and after few seconds (about 30 s from one image to another) to show the formation of rouleaux (left panel) and of RBCs at 25% and 45% suspended in ACD plus Albumin solution. Scale bar is 20 μm. Schematic drawings of RBCs rouleaux and cell shape in healthy conditions have been shown.

In particular, in the first set of experiments, the OECT response was visualized by applying sequences of V_{GS} pulses, with duration of 60 s and progressively-increasing amplitudes going from 0 to 0.6 V (step 0.1 V) at fixed drain-source voltage, $V_{DS} = -0.1$ V (Fig. 3a). The drain-source current (I_{DS}) and the corresponding gate-source current (I_{GS}) were thus recorded as a function of time. Hence, OECT current modulation capability could be expressed by the ratio, $\Delta I_{DS}/I_0$, derived from the pulsed measurements and described in detail elsewhere³¹ (Fig. 3b). Measurements in Fig. 3 confirm that, even in these complex media, OECTs operate correctly as depletion-mode transistors under the application of positive V_{GS} (i.e., I_{DS} is lowered in absolute value). It should be also mentioned that, in this case, the measurements were exploited up to $V_{GS} = 0.6$ V, due to the occurrence of device response degradation at larger V_{GS} (namely, the lack of the correct depletion-mode operation). While comparing the OECT responses in blood and plasma with gold electrodes, we notice that only small differences are appreciable mainly for V_{GS} between 0.2 and 0.5 V, with slightly enhanced current modulation values in blood. The strong similarity between the responses in these two fluids can be likely ascribed to the very large ionic concentrations in plasma.

ARTICLE

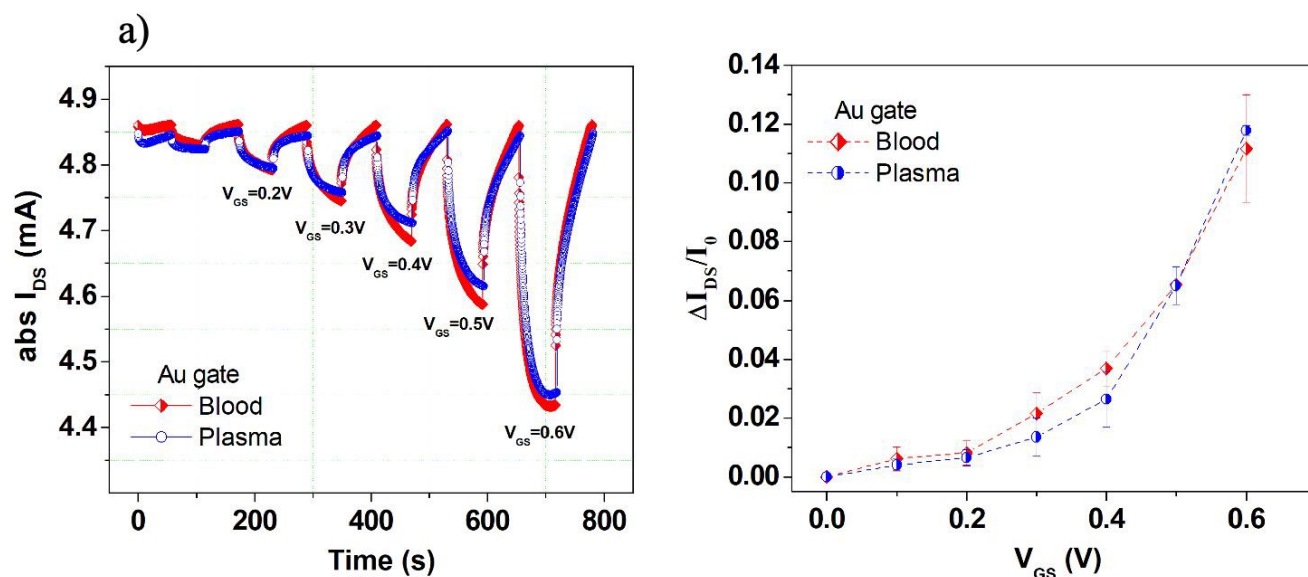


Fig. 3: OECT electrical response. a) Pulse reporting I_{DS} in absolute values as a function of time at V_{GS} from 0 to 0.6 V for plasma and whole blood using a gold gate. b) OECT modulation ratio ($\Delta I_{DS}/I_0$) as a function of V_{GS} for plasma and whole blood. The $\Delta I_{DS}/I_0$ values have been obtained as average of three consecutive measurements, with the error bars representing the standard deviation, in order to assess the device operation stability throughout the measurements.

In order to get additional insights about the OECT response in plasma and blood, the $I_{DS}(t)$ transient pulses, achieved with the gold electrode and for the different V_{GS} pulses, were further analyzed. Hence, these experimental curves were normalized with respect to the initial value and shifted at $t=0$ s. The obtained datasets are reported in Fig. 4a for whole blood and in Fig. 4b for plasma. Then, following the approach introduced in reference³¹, these data were fitted by using the double-exponential equation:

$$I_{DS}(t, V_{GS}) = I_{SS} + A_1 \cdot e^{-\left(\frac{t}{\tau_1}\right)} + A_2 \cdot e^{-\left(\frac{t}{\tau_2}\right)} \quad \text{eq. 1}$$

where I_{SS} is the current value at the end of the 60 s pulse, A_1 and A_2 are two pre-exponential factors and τ_1 and τ_2 are two time constants. The fitting parameters τ_1 and τ_2 of whole blood and

plasma represent mainly the OECT response for long and short times, respectively, and are reported in Fig. 4c.

For better clarity, a single $I_{DS}(t)$ pulse, compared with the related fitting curve, is shown (Fig. S2a) in the Supplementary material, where the overall behavior of A_1 and A_2 achieved for the whole set of transient measurements is also presented (Fig. S2b and c).

Appreciable differences between blood and plasma can be observed in Fig. S2b-c for the A_1 pre-factor with respect to A_2 one. In the case of τ_1 and τ_2 , for both time constants, blood experimental data provide higher values in the V_{GS} range between 0.2 and 0.5 V (Figs. 4c-d). As a whole, these data suggest that the OECT response in blood is able to get larger I_{DS} modulation but its dynamics as a function of the time is slightly slower if compared with the case of plasma.

ARTICLE

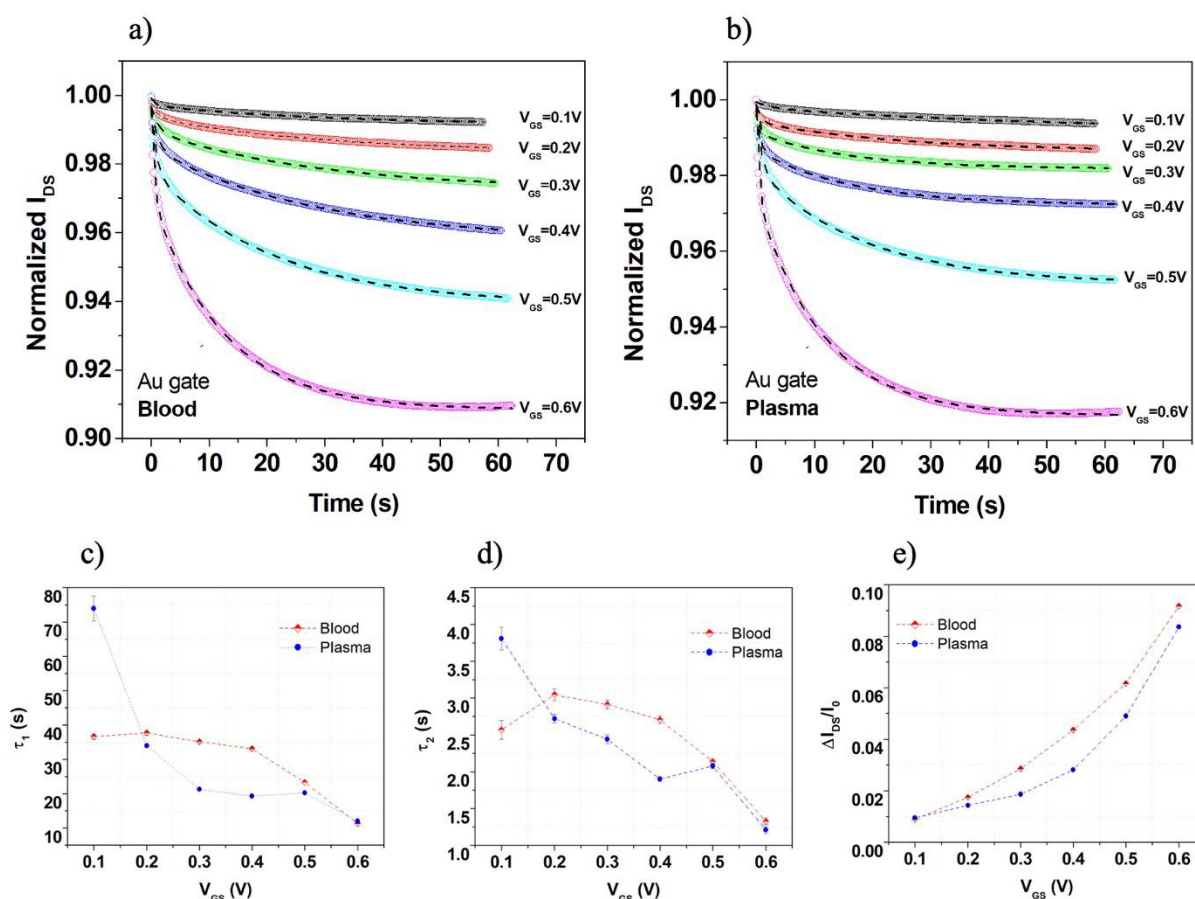


Fig. 4: a) Set of I_{DS} vs time curves (normalized to the initial value and time shifted at $t = 0$ s) recorded at different V_{GS} for blood and b) plasma using a gold gate. c) τ_1 and d) τ_2 time constants as a function of V_{GS} extracted by fitting experimental $I_{DS}(t)$ curves with the equation 1 for whole blood and plasma. e) OECT modulation ratio values estimated by the fitting procedure in the steady state conditions as a function of V_{GS} for plasma and whole blood.

As a further confirmation of this interpretation, in Fig. 4e we report the estimated current modulation at the end of the 60 s pulse conditions (i.e. derived from the I_{SS} fitting parameter in equation 1). Here, the enhanced current modulation capability in blood is still more evident than what observed in Fig. 3b.

As discussed in³¹, the larger values of τ_1 should be ascribed to the enhanced viscous character of whole blood⁴³. This type of observation is in qualitative agreement with a recently-proposed model where the diffusion of cations throughout the electrolytes was correlated to the solution viscosity, in analogy with Einstein-Smoluchowski theory⁴⁴. On the other hand, the short time constant τ_2 should be more related to the capacitive coupling between the ionic and electronic components of the overall system. In our experiments, in particular, by considering the size of the gate immersed area and the overall dimensions of the PEDOT:PSS channel with the related volumetric capacitance ($C_V \sim 40 \text{ F} \cdot \text{cm}^{-3}$),

we can infer that the OECT response is basically ruled by the electric double-layer (EDL) capacitance (C_G) at the gate-electrolyte interface (i.e. $C_G \ll C_V$)⁴⁵. In this scenario, the increased values of τ_2 (with V_{GS} between 0.2 and 0.5 V) for blood may be associated to larger values of C_G as a possible effect of the RBCs presence and related motion toward the gate surface.

As reported in literature^{46, 47}, the RBCs surface is negatively charged and hence, in an electrolytic solution, an electrical double layer is present also around the RBC. Under the effect of an external field (i.e. under positive V_G during the OECT operation) RBCs, with the surrounding charge layers and the related diffusive components, are attracted toward the gate electrode. As a whole, this effect should produce a local increase of the ionic concentrations close the gate surface, providing the final increase of C_G . Although this is a tentative explanation requiring additional and more specific experiments to be definitely proved, it is to be highlight how the

hypothesized C_G capacitance increase in blood vs plasma is compatible also with the observation of the corresponding larger gate current I_{GATE} values (see the data below referred to Fig. S3b). Given the polarizable nature of the gold electrode, in this case, a direct relation between the gate current and electrolyte-gate capacitive couplings is indeed expected.

Complementary experiments were also performed by using a platinum wire as gate electrode. In particular, Fig. S3 (Supplementary material) shows $I_{DS}(t)$ pulsed measurements achieved in this case for whole blood and plasma. As shown, the OECT responses with the platinum gate electrode are even more similar and no significant differences can be observed in terms of $\Delta I_{DS}/I_0$ values which are, however, larger (by a factor close to 2) than those measured with the gold electrode. These findings point out to the less polarizable nature of platinum if compared with gold, in agreement with other recent works where the occurrence of Faradaic reactions at the platinum surface was indeed exploited to develop specific sensing devices^{48–50}. In particular, the excellent electrocatalytic activity of Pt (even in form of nanoparticles incorporated in the PEDOT:PSS channel) toward H_2O_2 oxidation was exploited to demonstrate the efficient detection of neurotransmitters⁵¹. Overall, it is essential, indeed, to remind that the OECT response can be strongly affected by the physiochemical nature of the gate^{52,53}.

OECT response in ACD plus Albumin solutions

A second set of experiments was focused on the specific role of RBCs in the OECT response. For this reason, alternative electrolytic solutions able to preserve the initial healthy conditions of the erythrocytes were used. Hence, RBCs have been separated from whole blood by centrifugation and suspended again in a buffer solution made of ACD and Albumin⁵⁴ (see Material and methods section).

ACD is commonly employed as an anticoagulant to prevent the formation of cell aggregates and Albumin, being the most abundant protein of blood plasma, operates, in appropriate concentration, as nutrient for RBCs. ACD and Albumin supplemented ACD solutions have been used by the authors in other works^{18, 19, 55} and have been preliminarily tested here as electrolytes in the OECT (Fig. S4). As shown, ACD and ACD plus Albumin solutions show a very similar OECT response in terms of the current modulation capability, with the measured $\Delta I_{DS}/I_0$ values remaining remarkably smaller than those observed in plasma and blood (about by a factor 5 at $V_{GS}=0.6$ V). Fig. S4b shows also the I_{GATE} values achieved for ACD and ACD plus Albumin solutions in comparison again with blood and plasma. This trend reproduces very well that observed for the $\Delta I_{DS}/I_0$ values with the I_{GATE} being strongly reduced for the ACD and ACD plus Albumin solutions.

Once characterized in terms of their baseline OECT modulation signal, ACD plus Albumin solutions have been used as buffer to suspend RBCs. Two different RBCs concentrations, at 25% and

45% (the latter corresponding to the hematocrit in whole blood), were here considered.

DOI: 10.1039/D1TB01584B

In this regard, Fig. S5a shows the $\Delta I_{DS}/I_0$ modulation curves achieved for the whole blood, the basic ACD plus Albumin solution and for the same type of solution containing 25% and 45% of RBCs. These data outline unambiguously how the OECT response is affected by the presence of RBCs. In particular, the responses recorded in the solutions containing the two RBCs concentrations, 25 and 45% (the latter corresponding to whole blood *Hct*), exhibit an intermediate character in comparison with the whole blood and the basic suspending medium. I_{DS} modulation capability was somewhat enhanced for the larger RBCs concentration, at increasing V_{GS} (Fig. S5b).

In order to further analyze the OECT response in these fluids, transfer curves at $V_{DS}=0.1$ V were also recorded. In this case, the investigated V_{GS} range was extended up to 0.8 V without observing any degradation signature in the depletion-mode OECT response.

Normalized transfer curves, reporting the change in the device current I_{DS} normalized to the value measured at $V_{GS}=0$ V, are shown in Fig. 5a. Coherently with the features observed in the $\Delta I_{DS}/I_0$ curves (Fig. S5a), the responses recorded in the ACD plus Albumin solutions containing the two RBCs concentrations exhibit again an intermediate character. A more careful inspection of these measurements highlights also a different V_{GS} dependence. This specific behavior was better emphasized by analyzing the OECT transconductance ($g_m = \frac{\partial I_{DS}}{\partial V_{GS}}$), which is a very important parameter simply defined as the derivative of the channel current I_{DS} with respect to the gate voltage V_{GS} . In particular, such parameter describes the OECT signal amplification performances^{56, 57}. In Fig. 5b, transconductance (g_m) is plotted as a function of V_{GS} for all the solutions investigated and very different trends can be observed. Indeed, g_m rises at increasing V_{GS} for all fluids, but the specific V_{GS} value where this behavior starts and the presence of a peak, with the related magnitude, are characteristic of any solution.

In particular, three different regions can be identified:

- the low V_{GS} range (approximately up to $V_{GS}=0.3$ V) where all g_m curves assume values of few hundreds of μS , with a slight V_{GS} dependence. Here, the solutions containing RBCs seem to display smaller g_m even in comparison with the basic ACD plus Albumin suspending medium;
- the intermediate V_{GS} region (approximately between 0.3 and 0.6 V) where the g_m rising behavior is much more evident. In this case, in comparison with the ACD plus Albumin suspending medium, the presence and a major concentration of RBCs tend to reduce the V_{GS} threshold above which this trend is more pronounced.
- the high V_{GS} range (between 0.6 and 0.8 V), where, except for the basic ACD plus Albumin suspending medium, g_m exhibits a peak for all the solutions. Here, the ACD plus Albumin solutions with 25% and 45% RBC concentrations differ for both the peak amplitude and the V_{GS} value where this occurs.

Thus, the g_m behavior in the intermediate V_{GS} region, with higher trans-conductance for the ACD plus Albumin solution at 45% RBC concentration with respect to that at 25% RBC, seems suggesting again an increase of the capacitive coupling ($g_m \propto C_G$ since $C_G \ll C_V$) between the gold gate electrode and the electrolytic medium. This occurrence agrees well with the

abovementioned considerations about the OECT transient response in blood (i.e. larger values of the short time constant τ_2), pointing again at the role of negatively-charged RBC in enhancing the C_G value in the same V_G range.

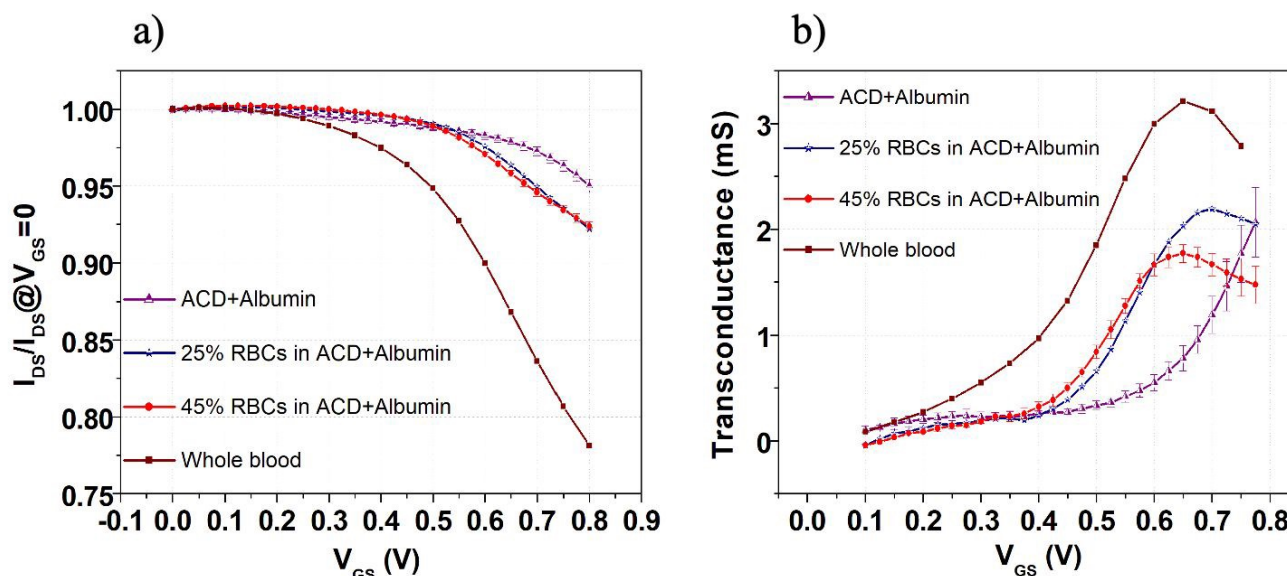


Fig. 5: a) Normalized transfer curves I_{DS}/I_{DS} at $V_{GS}=0$ V and b) transconductance as a function of V_{GS} for ACD plus Albumin, Plasma, RBCs at 45% in ACD plus Albumin and whole blood. V_{GS} is pulsed from 0 to 0.8 V and V_{DS} set at 0.1 V.

On the other hand, when V_{GS} values still increase (between 0.6V and 0.8V), the OECT response reaches a different regime where the major RBC concentration in ACD plus Albumin solutions provides a reduced I_{DS} modulation capability (i.e. the g_m peak amplitude is lowered and occurs at lower V_{GS}). This condition underlines a weaker penetration of cationic species into the PEDOT:PSS film and is compatible with a field effect-like operation mode localized at the PEDOT:PSS surface⁵⁸.

The physical interpretation of this phenomenon is not straightforward but it could be tentatively explained in terms of an increasing repulsion effect among the negatively-charged RBCs close the gold surface or to the detrimental occurrence of RBC sticking effects at the same surface. Both occurrences, indeed, could degrade the electric double layer formation and make ineffective the progressive enhancement of the gate signal in promoting a further cationic uptake by the active channel. It is worth to mention, in any case, that while it was previously shown that the position and magnitude of g_m peak in the OECT response can be tailored as a function of the device geometrical layout and/or the biasing conditions, here we found that these features can be clearly associated also to the nature of the analyzed electrolyte^{59, 60}.

As a final comment suggested by the data summarized in Fig.5, we want to highlight how the transconductance curves recorded for blood and ACD plus Albumin solution at 45% RBC

concentration display a very different behavior, even in presence of the same RBC concentration.

As above discussed, this finding was obviously related to the different suspending medium, but it is also a demonstration that the RBC sedimentation does not affect ion diffusion towards PEDOT:PSS channel. On the other hand, if RBC sedimentation on the PEDOT:PS surface was the dominant feature affecting the operation of OECT here investigated, higher I_{DS} modulation values would be expected for plasma in comparison with the whole blood. This occurrence was clearly not observed during our experiments.

3. Conclusions

In this work, OECTs based devices are exploited for the first time to study the electrical response of whole blood and RBC suspensions. The response of OECT in blood and plasma was analyzed by using both gold and platinum gate electrodes. While the OECT behavior with the platinum gate was found to be completely dominated by the strong ionic concentration related to plasma, with gold electrodes we were able to identify distinctive features of the OECT steady state and transient responses in blood and plasma. In a second set of experiments, aimed at separating the effect of plasma and RBCs by suspending RBCs, at different concentrations, in a buffer (ACD)

ARTICLE

Journal Name

supplemented with Albumin, we observed a clear difference in the response of OECTs. In particular, the latter was analyzed in terms of the transconductance (g_m) parameter extracted from transfer curve measurements. The role of negative charges distributed on the RBC surface has been tentatively invoked to explain the main findings here reported. Finally, RBCs morphology was monitored just after the withdrawal and during the electrical experiments and no alterations were observed. Indeed, microscopy observations show that, after the application of voltage to blood or RBC suspensions, no cell lysis or evident structural modifications can be observed, thus proving that OECTs are suitable tools for blood-based devices. In conclusions, despite the use of OECTs for blood sensing is far from straightforward due to the intrinsic complexity of blood and its components, these results could lead to the development of a new class of integrated devices suitable for drug testing and clinical diagnostics.

Acknowledgements

V. Preziosi gratefully acknowledges funding from the STAR Linea1/2018 project and funding from the FISIR 2020 project. The authors thank Iliana Espedito for her help in the electrical measurements during her master thesis.

Author Contributions: V.P., M.B. and G.T. conceived the project. M.B. and V.P. performed OECT measurements. V.P. and G.T. performed conductivity measurements and acquired microscopy images. A.V. and M.C. designed the OECT and realized the electrodes photolithographic masks. S.M., A.V. and P.D. realized OECT devices and performed some of the OECT experiments. S.G. and A.C. contributed to the discussion and reviewed the manuscript. All the authors discussed results. V.P. and M.B. wrote the manuscript.

Author Information: Reprints and permissions information is available at ...The authors declare no competing financial interests. Correspondence and requests for materials should be addressed to mario.barra@spin.cnr.it and valentina.preziosi@unina.it.

Supplementary Material is available in the online version of the paper.

References

1. V. F. Curto, B. Marchiori, A. Hama, A.-M. Pappa, M. P. Ferro, M. Braendlein, J. Rivnay, M. Flocchi, G. G. Malliaras and M. Ramuz, *Microsystems & nanoengineering*, 2017, **3**, 1-12.
2. S. Ricci, S. Casalini, V. Parkula, M. Selvaraj, G. D. Saygin, P. Greco, F. Biscarini and M. Mas-Torrent, *Biosensors and Bioelectronics*, 2020, **167**, 112433.
3. S. Y. Yang, J. A. DeFranco, Y. A. Sylvester, T. J. Gobert, D. J. Macaya, R. M. Owens and G. G. Malliaras, *Lab on a Chip*, 2009, **9**, 704-708.
4. D. Ohayon and S. Inal, *Advanced Materials*, 2020, **32**, 2070267.
5. D. A. Bernards and G. G. Malliaras, *Advanced Functional Materials*, 2007, **17**, 3538-3544.
6. F. Torricelli, D. Z. Adrahtas, Z. Bao, M. Berggren, F. Biscarini, A. Bonfiglio, C. A. Bortolotti, C. D. Frisbie, E. Macchia and G. G. Malliaras, *Nature Reviews Methods Primers*, 2021, **1**, 1-24.
7. Y. Lee and T.-W. Lee, *Accounts of chemical research*, 2019, **52**, 964-974.
8. D.-G. Seo, G.-T. Go, H.-L. Park and T.-W. Lee, *MRS Bulletin*, 2021, 1-9.
9. A. Spanu, L. Martinez and A. Bonfiglio, *Lab on a Chip*, 2021, **21**, 795-820.
10. J. Rivnay, S. Inal, A. Salleo, R. M. Owens, M. Berggren and G. G. Malliaras, *Nature Reviews Materials*, 2018, **3**, 17086.
11. J. Rivnay, R. M. Owens and G. G. Malliaras, *Chemistry of Materials*, 2013, **26**, 679-685.
12. X. Strakos, M. Bongo and R. M. Owens, *Journal of Applied Polymer Science*, 2015, **132**, 41735.
13. R. M. Owens and G. G. Malliaras, *MRS bulletin*, 2010, **35**, 449-456.
14. C. Y. Chan, P.-H. Huang, F. Guo, X. Ding, V. Kapur, J. D. Mai, P. K. Yuen and T. J. Huang, *Lab on a Chip*, 2013, **13**, 4697-4710.
15. A. D. van der Meer and A. van den Berg, *Integrative Biology*, 2012, **4**, 461-470.
16. N. S. Bhise, J. Ribas, V. Manoharan, Y. S. Zhang, A. Polini, S. Massa, M. R. Dokmeci and A. Khademhosseini, *Journal of Controlled Release*, 2014, **190**, 82-93.
17. R. Hoffman, E. J. Benz Jr, L. E. Silberstein, H. Heslop, J. Anastasi and J. Weitz, *Hematology: basic principles and practice*, Elsevier Health Sciences, 2013.
18. G. Tomauiuolo, M. Barra, V. Preziosi, A. Cassinese, B. Rotoli and S. Guido, *Lab Chip*, 2011, **11**, 449-454.
19. G. Tomauiuolo, M. Simeone, V. Martinelli, B. Rotoli and S. Guido, *Soft Matter*, 2009, **5**, 3736-3740.
20. S. Shattil, B. Furie, H. Cohen, L. Silverstein, P. Glave and M. Strauss, *Churchill Livingstone, Philadelphia*, 2000.
21. M. Diez-Silva, M. Dao, J. Han, C.-T. Lim and S. Suresh, *MRS bulletin*, 2010, **35**, 382-388.
22. V. Acharya and P. Kumar, 2017, *Frontiers in microbiology*, 2017, **8**, 889.
23. G. Tomauiuolo, *Biomicrofluidics*, 2014, **8**, 051501.
24. H. Krebs, *Annual review of biochemistry*, 1950, **19**, 409-430.
25. J. Schaller, S. Gerber, U. Kaempfer, S. Lejon and C. Trachsel, *Human blood plasma proteins: structure and function*, John Wiley & Sons, 2008.
26. J. C. Maxwell, *A treatise on electricity and magnetism*, Oxford: Clarendon Press, 1873.
27. H. Fricke, *Physical Review*, 1924, **24**, 575.
28. S. Velick and M. Gorin, *The Journal of general physiology*, 1940, **23**, 753.
29. K. R. Visser, 1989, *Images of the Twenty-First Century. Proceedings of the Annual International Engineering in Medicine and Biology Society*, 1989, **5**, 1540-1542.
30. F. G. Hirsch, E. C. Texter Jr, L. A. Wood, W. C. Ballard Jr, F. E. Horan, I. S. Wright, C. Frey and D. Starr, *Blood*, 1950, **5**, 1017-1035.
31. V. Preziosi, M. Barra, A. Perazzo, G. Tarabella, R. Agostino, S. L. Marasso, P. D'Angelo, S. Iannotta, A. Cassinese and S. Guido, *Journal of Materials Chemistry C*, 2017, **5**, 10.
32. V. Preziosi, G. Tarabella, P. D'Angelo, A. Romeo, M. Barra, S. Guido, A. Cassinese and S. Iannotta, *RSC Advances*, 2015, **5**, 8.
33. D. Gentili, P. D'Angelo, F. Militano, R. Mazzei, T. Poerio, M. Brucale, G. Tarabella, S. Bonetti, S. L. Marasso and M. Cocuzza, *Journal of Materials Chemistry B*, 2018, **6**, 5400-5406.
34. G. Tarabella, A. G. Balducci, N. Coppedè, S. Marasso, P. D'Angelo, S. Barbieri, M. Cocuzza, P. Colombo, F. Sonvico and R. Mosca, *Biochimica et Biophysica Acta (BBA)-General Subjects*, 2013, **1830**, 4374-4380.
35. P. D'Angelo, G. Tarabella, A. Romeo, A. Giodice, S. Marasso, M. Cocuzza, F. Ravanetti, A. Cacchioli, P. G. Petronini and S. Iannotta, *MRS Communications*, 2017, **7**, 229-235.
36. G. Tarabella, S. L. Marasso, V. Bertana, D. Vurro, P. D'Angelo, S. Iannotta and M. Cocuzza, *Materials*, 2019, **12**, 1357.
37. P. D'Angelo, G. Tarabella, A. Romeo, S. Marasso, M. Cocuzza, C. Peruzzi, D. Vurro, G. Carotenuto and S. Iannotta, 2018, **1990**, 020015.
38. V. Introini, A. Carciati, G. Tomauiuolo, P. Cicutta and S. Guido, *Journal of the Royal Society Interface*, 2018, **15**, 20180773.
39. L. Lanotte, G. Tomauiuolo, C. Misbah, L. Bureau and S. Guido, *Biomicrofluidics*, 2014, **8**, 014104.
40. A. Zhanov and S. Yang, *PLoS One*, 2015, **10**, e0129337.
41. V. A. Battistoni Silvia, Marasso Luigi Simone, Cocuzza Matteo, Erokhin Victor, *Physica Status Solid*, 2020, **217**.
42. H. Bäuml, B. Neu, E. Donath and H. Kieseewetter, *Biorheology*, 1999, **36**, 439-442.
43. R. E. Wells and E. W. Merrill, *The Journal of clinical investigation*, 1962, **41**, 1591-1598.
44. N. Coppedè, M. Villani and F. Gentile, *Scientific reports*, 2014, **4**.
45. J. T. Friedlein, R. R. McLeod and J. Rivnay, *Organic Electronics*, 2018, **63**, 398-414.
46. K.-M. Jan and S. Chien, *Journal of General Physiology*, 1973, **61**, 638-654.
47. H. P. Fernandes, C. L. Cesar and M. d. L. Barjas-Castro, *Revista brasileira de hematologia e hemoterapia*, 2011, **33**, 297-301.
48. H. Tang, P. Lin, H. L. Chan and F. Yan, *Biosensors and Bioelectronics*, 2011, **26**, 4559-4563.
49. D. J. Macaya, M. Nikolou, S. Takamatsu, J. T. Mabeck, R. M. Owens and G. G. Malliaras, *Sensors and Actuators B: Chemical*, 2007, **123**, 374-378.
50. G. Tarabella, A. Pezzella, A. Romeo, P. D'Angelo, N. Coppedè, M. Calicchio, M. D'Ischia, R. Mosca and S. Iannotta, *Journal of Materials Chemistry B*, 2013, **1**, 3843-3849.
51. L. Kergoat, B. Piro, D. T. Simon, M. C. Pham, V. Noël and M. Berggren, *Advanced Materials*, 2014, **26**, 5658-5664.

Journal Name

ARTICLE

52. G. Tarabella, C. Santato, S. Y. Yang, S. Iannotta, G. G. Malliaras and F. Ciccoira, *Applied Physics Letters*, 2010, **97**, 123304.
53. P. Lin, F. Yan and H. L. Chan, *ACS applied materials & interfaces*, 2010, **2**, 1637-1641.
54. J. N. Mulvihill, A. Faradji, F. Oberling and J. P. Cazenave, *Journal of biomedical materials research*, 1990, **24**, 155-163.
55. R. D'Apolito, G. Tomaiuolo, F. Taraballi, S. Minardi, D. Kirui, X. Liu, A. Cevenini, R. Palomba, M. Ferrari and F. Salvatore, *Journal of Controlled Release*, 2015, **217**, 263-272.
56. D. Khodagholy, J. Rivnay, M. Sessolo, M. Gurfinkel, P. Leleux, L. H. Jimison, E. Stavrinidou, T. Herve, S. Sanaur and R. M. Owens, *Nature communications*, 2013, **4**, 1-6.
57. E. Macchia, P. Romele, K. Manoli, M. Ghittorelli, M. Magliulo, Z. M. Kovács-Vajna, F. Torricelli and L. Torsi, *Flexible and Printed Electronics*, 2018, **3**, 034002.
58. E. Zeglio and O. Inganäs, *Advanced Materials*, 2018, **30**, 1800941.
59. J. Rivnay, P. Leleux, M. Sessolo, D. Khodagholy, T. Hervé, M. Focchi and G. G. Malliaras, *Advanced Materials*, 2013, **25**, 7010-7014.
60. J. Nissa, P. Janson, D. T. Simon and M. Berggren, *Applied Physics Letters*, 2021, **118**, 053301.

View Article Online
DOI: 10.1039/D1TB01584B